ADAPTIVE DIGITAL FILTERING FOR ULTRASONIC STRAIN-FLOW IMAGING

Christian Kargel*, Michael F. Insana‡
*Department of Medical Information Technology, Carinthia Tech Institute,
University of Applied Sciences, Klagenfurt, Austria
‡Department of Biomedical Engineering, University of California Davis, USA
Email: c.kargel@cti.ac.at; mfinsana@ucdavis.edu

Abstract

This paper presents results for a strain-flow imaging system recently developed to improve detection of early cancer by simultaneously imaging tissue elasticity and vascular blood flow. The main challenge in strain-flow imaging is to separate echo signal components caused by blood flow from tissue motion components that vary spatially and temporally. In tumor imaging the blood velocity can be relatively slow thus producing a low mean-frequency Doppler spectrum. This often results in a spectral overlap with echos from tissue motion and considerably complicates the efficient separation of the two components. We shall demonstrate that a digital eigenfilter adaptive to the tissue echo signal statistics performs very well for this task. Due to the excellent performance of this type of filtering we are able to obtain accurate and precise velocity estimates in strain-flow environments when using a two-dimensional (2D) autocorrelator approach. Furthermore, crosscorrelation-based tissue strain imaging is improved because strain decorrelation noise due to flow components is virtually eliminated resulting in high-quality strain-flow imaging.

Introduction

Strain-flow (SF) imaging is a new method for imaging vascularization and perfusion of e.g. metastatic tumors while assessing viscoelastic properties and may improve our understanding of tumor development. It is well known that neoplasms have increased vascularity to supply fast-growing tissues with nutrients [1]. Concurrently, these tissues undergo structural remodeling causing them to stiffen due to hyperplasia, fibrosis [2], and desmoplasia [3]. To overcome the restrictions imposed by commercial ultrasound scanners, we developed a flexible laboratory imaging system specifically to investigate tumor vasculature and elasticity, simultaneously, in small animal tumor models.

At ultrasonic frequencies below 20 MHz it is very challenging to separate small-amplitude blood flow echo signals from large-amplitude tissue echos (clutter). Additionally, in tumor imaging the tissue motion and blood flow signal components often lie in the same Doppler frequency band. Due to this Doppler frequency overlap, conventional high-pass clutter rejection filtering only provides moderate performance. Adaptive eigenfilters were shown to be superior in suppressing tissue echos compared with various conventional clutter rejection filters implemented in commercial ultrasound scanners [4], [5]. We adopted the eigenfilter approach with some modifications for strain-flow imaging. To achieve high-quality blood flow velocity estimates we use an extension of the well-known Kasai autocorrelator [6]. Strain estimation is performed by a crosscorrelation-based technique applied in strain imaging for many years [7]. Experimental evaluation of the new approach is performed by using our laboratory strain-flow imaging system [8] and a tissue-mimicking flow phantom.

Strain-Flow Imaging and Filtering

In conventional color-flow imaging (CFI) echo signals from tissues are considered a nuisance and discarded. However, these signals convey information about the displacement and elasticity surrounding the vessel lumen. Conventional strain imaging utilizes single pulse returns per line-of-sight (LOS) at different tissue compressions whereas CFI usually uses multiple echo signals per LOS. High precision strain estimates require the application of broadband pulse transmission to minimize the amount of tissue deformation that occurs on the scale of the pulse volume. In contrast, most precise blood flow velocity estimates are obtained with narrowband pulses and large packet sizes, provided larger vessels with steady flow are probed. In situations like tumor imaging where the flow is spatially disorganized and can be pulsatile, the pulsing requirements for the two methods naturally converge. The pulse bandwidth must be appropriately chosen to minimize strain-flow estimation errors for the specific imaging situation. Strain and blood velocity can then be estimated from the same echo data set. For other applications where the highest estimation performances are required, separate pulse packets for strain and flow estimation with 2 different bandwidths can be interleaved at the expense of higher frame rates.

The separation of blood flow and tissue motion signal components from ultrasound echos is essential in strain-flow imaging since signal components that carry strain information produce artifacts in flow estimation and vice versa. In many situations tissue motion and blood flow signals are largely complementary and a single strain-flow filter is able to successfully separate the two components of motion (Fig. 1). Thus the typical highpass clutter rejection filter effective for CFI provides the design for how to filter for strain: the complement of the clutter rejection filter output represents the lowpass filtered signal necessary for strain imaging. However, strain estimation using the filter complement can be very much influenced by the filter response ripples which, for tissue clutter signals, appear in the passband. For example, a Chebyshev type II HP filter (with equal amplitude ripples in the stopband) can be effective to suppress clutter for velocity estimation but the quality of the filter complement signal is insufficient for strain estimation. In such situations or when the echo signal also includes

non-physiological motion, e.g. transducer motion, two parallel filters must be designed.

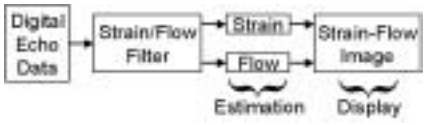

Figure 1: Combined strain-flow imaging and filtering.

We adopted the eigenfilter approach for strain-flow imaging and shall show that the quality of strain estimates can be significantly improved by applying a single adaptive eigenfilter optimized for clutter suppression in CFI.

Adaptive Eigenfilters

Clutter rejection filtering includes the application of conventional FIR and IIR filters, the latter with various initialization techniques to minimize transient filter responses, polynomial regression filters, and, more recently, adaptive eigenfilters. A review of principles, comparisons of filter frequency responses and performance evaluations can be found in [4], [5]. It is shown that eigenfilters provide superior performance in CFI at the cost of a somewhat increased computational load. For most complex imaging situations usually existent in strain-flow environments, the filtering must exhibit maximum performance and adaptability. Traditional highpass clutter rejection filters only provide moderate performance, largely due to the spectral overlap of tissue motion and blood flow echo signals. Furthermore, these filters are usually designed with real filter coefficients and thus respond symmetrically. We recently demonstrated that asymmetric frequency responses and characteristics other than highpass can be easily realized with properly designed eigenfilters [9]. These features are needed when tissue and blood velocities have the same order of magnitude but opposite signs (directions) or when tissue velocity is higher than blood velocity.

Eigenfilter Design

Digitized echo signals are usually organized in 2D arrays at every LOS where the terms "fast-time" (columns) and "slow-time" (rows) define the direction of the ultrasound beam axis ($m = 1 \dots M$) and pulse packet dimension ($n = 1 \dots N$), respectively. M is the number of depth samples and N the number of pulse transmissions at a given LOS. Clutter rejection and strain-flow filters operate in slow-time dimension, i.e. based on the temporal echo signal samples of multiple pulse transmissions (index n) from fixed depth positions (index m).

A linear filtering operation can generally be expressed as $\mathbf{y} = \mathbf{A}\mathbf{x}$, where $\mathbf{x}$ is the complex (slow-time) input signal vector, $\mathbf{y}$ is the complex output vector, both of dimension $N \times 1$, and $\mathbf{A}$ is an $N \times N$ dimensional filter matrix,

$$\mathbf{A} = \mathbf{I} - \sum_{k=1}^{K} \mathbf{b}_k \, \mathbf{b}_k^H \; . \tag{1}$$

$\mathbf{b}_k$ is the set of basis vectors, $(\dots)^H$ the Hermitian operator, and $\mathbf{I}$ the identity matrix. The eigenfilter approach is to create a unique set of basis vectors for a specific tissue motion (clutter) space that adapts to the statistics of that clutter signal. The Hotelling transform[1] decomposes the echo data vector $\mathbf{x}$ into N orthogonal eigenvectors $(\mathbf{e}_1, \dots, \mathbf{e}_N)$ of the clutter covariance matrix[2]

$$\mathbf{C}_C = \mathcal{E}\{\mathbf{x}\,\mathbf{x}^H\}\,, \tag{2}$$

where $\mathcal{E}\{\cdot\}$ is the expected value. In the common situation where echo-signal energy from tissue is much greater than from blood flow, the largest eigenvalues correspond to the tissue component. The corresponding eigenvectors are arranged in descending order of energy such that a first-order eigenfilter ($K = 1$) is implemented by subtracting the first eigencomponent (highest energy) from the input signal. Second-order eigenfilters ($K = 2$) subtract the highest and second highest energy components.
While echos from tissues are usually contained in a subspace defined by $(\mathbf{e}_1, \dots, \mathbf{e}_K)$ with $K < N$, white noise is spread over all eigencomponents. Prior to blood velocity estimation all subspace eigencomponents that contain tissue echos and noise should be subtracted.

In practice, $\mathbf{C}_C$ is unknown a priori but can be estimated from the data by spatial averaging in depth direction:

$$\hat{\mathbf{C}}_C = \frac{1}{M'} \sum_{m=1}^{M'} \mathbf{x}_m \, {\mathbf{x}_m}^H \quad . \tag{3}$$

While temporal stationarity in slow-time is unnecessary, wide-sense stationarity in fast-time (depth) is needed for the estimation of $\hat{\mathbf{C}}_C$, and the depth region ($M' \leq M$) for averaging must be chosen appropriately. After computing the basis (eigen-) vectors from $\hat{\mathbf{C}}_C$, Eq. 1 is used to calculate the filter matrix $\mathbf{A}$.

Blood Flow Velocity Estimation

The well-known Kasai autocorrelator (AC) [6] is implemented in the vast majority of commercial scanners. It measures blood flow velocity by estimating the average phase shift with respect to the mean radio frequency (MRF) of the transmitted pulses between consecutive echo signals in slow-time for given depth locations along the fast-time axis. It is one-dimensional (1D) in the sense that estimation occurs along the slow-time axis.

The Kasai AC estimates the mean Doppler frequency (MDF) while assuming the MRF to be constant. However, the broadband pulse transmission required to obtain high spatial resolution coupled with frequency-dependent attenuation in tissues leads to estimation bias. Also, the stochastic nature of the scattered pressure field produces frequency fluctuations. As a result, the uncertainty in MDF measurements increases even for noiseless signals where flow is constant with time.

The 2D AC overcomes these drawbacks with its ability to estimate both mean frequencies, MDF and MRF, within each range gate. The estimator is two-dimensional in the sense that echo data are processed in

[1] The analogous transformation for transforming continuous data is named after the inventors Karhunen and Loéve.

[2] Covariance and correlation matrices are equal for zero-mean complex Gaussian random processes.

both the slow-time and fast-time dimensions. When analyzed in two dimensions a full evaluation of the classic Doppler equation is possible. As a result, velocity bias is greatly reduced and precision is consistently higher when a moderate increase in computational load is acceptable [10], [8]. However, the superiority of the 2D AC is diminished when the velocity spread inside the range gate is large or the echo SNR is low. Both weaken the correlation between MDF and MRF fluctuations that is necessary to improve precision.

The axial component v_a of the velocity vector in ultrasound beam direction can be estimated using the complex 2D autocorrelation function $\hat{R}(k,\ell)$ at lags $(k,\ell)=(0,1)$ and $(k,\ell)=(1,0)$ [10]:

$$v_a = \frac{c}{2}\frac{\frac{f_{PRF}}{2\pi}\arctan\left(\frac{\Im[\hat{R}_{2D}(0,1)]}{\Re[\hat{R}_{2D}(0,1)]}\right)}{f_{dem}+\frac{f_s}{2\pi}\arctan\left(\frac{\Im[\hat{R}_{2D}(1,0)]}{\Re[\hat{R}_{2D}(1,0)]}\right)}, \qquad (4)$$

where c is the longitudinal speed of sound, f_{PRF} the pulse repetition frequency, $\Re$ and $\Im$ denote the real and imaginary parts, f_{dem} is the demodulation frequency used for quadrature downmixing and f_s the sampling rate in fast-time.
$\hat{R}_{2D}$ is an estimate of the 2D autocorrelation function computed from the in-phase $I(m,n)$ and quadrature-phase $Q(m,n)$ components of the complex baseband echo signal:

$$\hat{R}_{2D}(k,\ell) = \sum_{m=0}^{M-k-1}\sum_{n=0}^{N-\ell-1}[I(m,n)+jQ(m,n)]\cdot \cdot[I(m+k,n+\ell)-jQ(m+k,n+\ell)].$$

Fig. 2 compares estimation performances of the Kasai and 2D ACs applied to the same IQ data set (SNR = 20 dB), modeling a constant velocity field ($v_a = 5.92$ mm/s; $c = 1480$ m/s) when a center frequency downshift from 15 MHz to 14 MHz occurred due to frequency-dependent tissue attenuation. Each echo signal in the pulse packet ($N = 8$) was divided into 100 range gates with lengths matched to the −20 dB transmit pulse duration (0.512 μs or 64 samples at $f_s = 125$ MS/s).

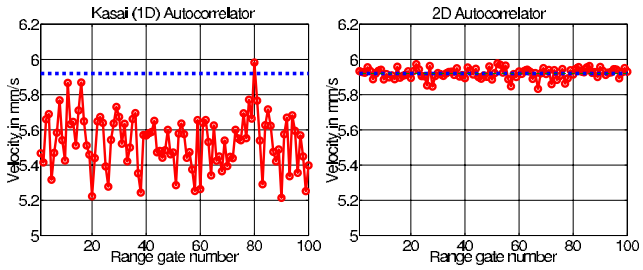

Figure 2: The broken horizontal lines indicate the true velocity. Only the 2D AC provides unbiased measurements (5.92±0.0287 mm/s), and the standard deviation σ_{v_a} in this specific situation is approx. 5× lower than for the Kasai AC,(5.533±0.1512) mm/s.

The results clearly demonstrate that the 2D AC significantly reduces the velocity bias in dispersive media with physiological attenuation as well as the velocity variance. Thus it is an excellent choice for real-time ultrasonic CFI and SF imaging. More detailed error analysis of both autocorrelators can be found in [8].

Strain estimation

Strain images are usually formed from crosscorrelation-based displacement estimates. Spatial derivatives yield strain estimates that then describe tissue or vascular elasticity. We often apply the Chaturvedi algorithm which employs local and global echo signal companding and determines local displacements at 3 spatial scales [7].

In blood flow imaging multiple echos are acquired at every LOS. When also using these echo signal packets in strain imaging, the quality of strain estimates can be improved by temporal averaging at the cost of a lower frame rate compared with conventional strain imaging that utilizes single echo signals at different compressions instead of pulse packets. However, acquisition frame rate is not decreased in combined strain-flow tumor imaging and simply determined by the acquisition time for the echo packet that is needed for blood flow estimation. Strain imaging then just takes advantage of the additional data already acquired. Any reduction in frame rate is caused solely by increased strain computation time. In some dynamic situations where processing must be fast we therefore apply autocorrelation-based strain estimation techniques.

It is also important to note that a properly-designed eigenfilter has virtually no influence on the fast-time tissue echo signal bandwidth [9]. Since the precision of crosscorrelation-based measurements increases with larger bandwidth, strain estimates are negligibly degraded when using eigenfilters.

Experimental Results

To study the performance of adaptive eigenfilters in strain-flow imaging we performed the following experiment: a soft tissue-mimicking graphite-gelatin phantom (elastic modulus 18 kPa) was constructed with two wall-less cylindrical flow channels. A blood-like scattering fluid – a 1% by mass suspension of cornstarch in water – flowed through the channels.
The first channel (3 mm diameter) was connected to an infusion pump that generated steady Poiseuille flow with a maximum velocity of the parabolic flow-profile in the center of the channel of about 15 mm/s while the gelatin of course was motionless. The second channel (5 mm diameter) was connected to a peristaltic pump (5 pulses/s) to produce cyclic motion in the gelatin and also modulated the previously steady flow in the first channel. This set-up with two adjacent channels allows the generation of tissue motion at approximately the same velocity as the flow which provides the greatest challenge for the strain-flow filter.

Data were acquired in M–mode from above the center of the 3-mm-channel using our laboratory scanner and a single-element, spherically-focused transducer (12.7 mm diameter, 15 MHz, f/3.5). Fig. 3 (left side) depicts the velocity map calculated by the 2D AC. Gelatin velocities ranged between ±5 mm/s, and flow in the 3-mm-channel was temporally modulated where the velocities ranged from $(-1\ldots30)$ mm/s. The softer flow channel strained more than the surrounding gelatin so a larger velocity modulation in the channel is to be expected.

Fig. 3 (right side) shows the velocities after a first-order eigenfilter ($N = 8$) was applied to separate flow components from tissue motion: flow inside the channel is barely influenced while tissue motion is completely eliminated.

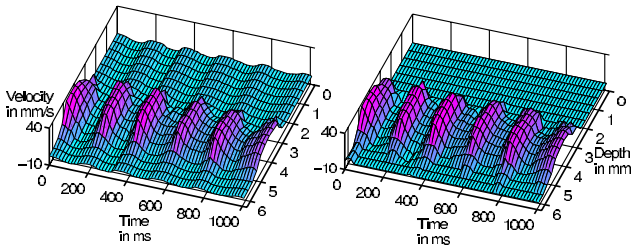

Figure 3: Flow and tissue velocities before (left) and after applying a first-order eigenfilter (right), see text.

Fig. 4 compares displacement and strain images obtained from the crosscorrelator before and after applying the eigenfilter. The top left image in Fig. 4 shows unfiltered displacement estimates. Fluid flow minimizes the inter-frame correlation coefficient between echoes in the flow channel, which gives the intense decorrelation noise. The upper right image is displacement computed

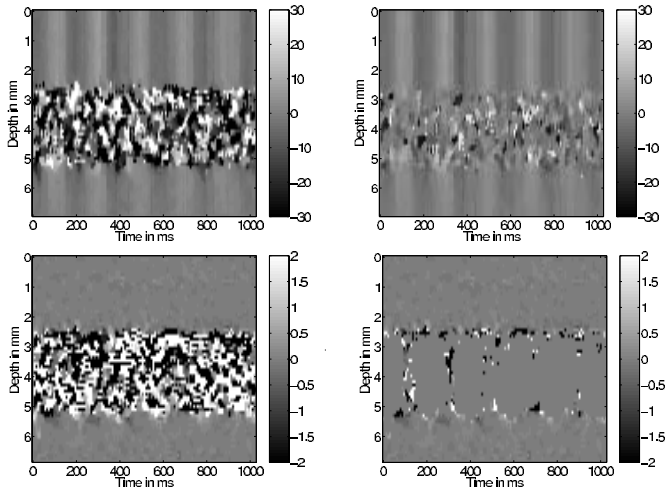

Figure 4: Displacement and strain images of M–mode data before (left) and after (right) application of a first-order eigenfilter (see text). The colorbars are scaled in microns (top row) and percent (bottom row).

from the tissue motion component alone, isolated from the same echo data by the eigenfilter. Decorrelation noise in the channel is significantly reduced by eliminating much of the flow- and noise-component signal energy while the estimation of tissue displacement is not influenced.

The lower left image of Fig. 4 shows strain derived from the upper left displacement image. Unfortunately, the axial displacement in the gelatin was virtually constant hence axial strain is zero, resulting in a uniform gray level outside the flow channel.

Deriving strain from the eigenfiltered displacement image (upper right) and masking all pixels marked for flow velocity estimation by the eigenfilter (Fig. 3, right) finally gives the image on the bottom right. Due to the eigenfilter most of the strain decorrelation noise is eliminated. If further reduction is needed, simple image processing can now be applied (e.g. median filtering). This would not be a successful approach without having applied the strain-flow eigenfilter.

Conclusions

We showed that an extension of the well-known Kasai autocorrelator can significantly improve the quality of flow estimation. We also demonstrated the excellent performance of an adaptive digital eigenfilter for the discrimination of flow and tissue motion signal components even if the corresponding velocities lie in the same Doppler frequency band. In situations where strain and flow components are largely complementary, isolation of the flow component by the eigenfilter also yields the tissue motion component with no further processing.

This phantom study shows that strain-flow imaging quality can be improved with only a moderate increase in computational load, facilitating high-quality strain-flow imaging in vivo for vascular applications.

References

[1] I. Wu and M.A. Moses, "Angiogenic molecules and mechanisms in breast cancer," Curr Oncol Rep, vol. 2, no. 6, pp. 566-571, 2000.

[2] T. Hasebe, K. Mukai, H. Tsuda, A. Ochial, "New prognostic histological parameter of invasive ductal carcinoma of the breast," Path Int, vol. 50, pp. 263-272, 2000.

[3] R. A. Walker, "The complexities of breast cancer desmoplasia," Breast Cancer Res, vol. 3, no. 3 pp. 143-145, 2001.

[4] S. Bjærum, H. Torp, K. Kristoffersen,"Clutter filter design for ultrasound color flow imaging," IEEE Trans Ultrason Ferro Freq Contr (TUFFC), vol. 49, no. 2, 2002.

[5] S. Bjærum, H. Torp, K. Kristoffersen, "Clutter filters adapted to tissue motion in ultrasound color flow imaging," IEEE TUFFC, vol. 49, no. 6, 2002.

[6] C. Kasai, K. Namekawa, A. Koyano, R. Omoto, "Real-time two-dimensional blood flow imaging using an autocorrelation technique," IEEE Trans Son Ultrason, vol. SU-32, no. 3, 1985.

[7] P. Chaturvedi, M. F. Insana, T. J. Hall, "Testing the limitations of 2-D local companding in strain imaging using phantoms," IEEE TUFFC, vol. 45, pp. 1022-1031, 1998.

[8] Ch. Kargel, G. Plevnik, B. Trummer, M. F. Insana, "Ultrasonic Visualization of Tumor Blood Flow," submitted to IEEE Trans Instrum Meas, July 2002.

[9] Ch. Kargel, G. Höbenreich, B. Trummer, M. F. Insana, "Adaptive Clutter Rejection Filtering in Ultrasonic Strain-Flow Imaging," IEEE TUFFC, vol. 50, no.7, pp. 824-834, 2003.

[10] T. Loupas, R. B. Peterson, R. W. Gill, "Experimental Evaluation of Velocity and Power Estimation for Ultrasound Blood Flow Imaging by Means of a Two-Dimensional Autocorrelation Approach," IEEE TUFFC, vol. 42, no. 4, 1995.